

## Supplementary Materials for

### **Human Neural Stem Cells Induce Functional Myelination in Mice with Severe Dysmyelination**

Nobuko Uchida,\* Kevin Chen, Monika Dohse, Kelly D. Hansen, Justin Dean, Joshua R. Buser, Art Riddle, Douglas J. Beardsley, Ying Wan, Xi Gong, Thuan Nguyen, Brian J. Cummings, Aileen J. Anderson, Stanley J. Tamaki, Ann Tsukamoto, Irving L. Weissman, Steven G. Matsumoto, Larry S. Sherman, Christopher D. Kroenke, Stephen A. Back\*

\*To whom correspondence should be addressed. E-mail: nobuko.uchida@stemcellsinc.com (N.U.); backs@ohsu.edu (S.A.B.)

Published 10 October 2012, *Sci. Transl. Med.* **4**, 155ra136 (2012)

DOI: 10.1126/scitranslmed.3004371

#### **The PDF file includes:**

##### Materials and Methods

Table S1. Antibodies used for histological and immunohistochemical studies.

Fig. S1. HuCNS-SC characteristics before and after transplantation.

Fig. S2. Production of myelin from 10 different HuCNS-SC lots.

Fig. S3 Time course of HuCNS-SC engraftment and oligodendrocyte differentiation in vivo.

Fig. S4. Juvenile transplantation of HuCNS-SCs.

Fig. S5. Microglia activation status of chronic transplants in *Shi-id* mouse brains.

Fig. S6. CAP recordings.

Fig. S7. Representative MRI images and analyses in the *Shi-id* mouse transplanted with HuCNS-SCs.

## Materials and Methods

### Generation of *Shi-id* mice

All animal housing conditions and surgical procedures were approved by and conducted according to the Institutional Animal Care and Use Committee at StemCells, Inc. *Shi* mice (C3Fe.SWV-*Mbp*<sup>shi</sup>/J) were from the Jackson Laboratory. The MBP<sup>shi</sup> mutation was backcrossed for 10 generations onto the NOD-*scid* background (*Shiverer-Nscid*). Alternatively, C3Fe.SWV-*Mbp*<sup>shi</sup>/J mice were backcrossed with *Rag2/IL-2R $\gamma$*  (RG) knockout mice for two generations and screened for homozygosity to *Mbp*<sup>shi</sup>, *Rag2*<sup>-/-</sup>, and X-linked *IL-2R $\gamma$*  mutations (*Shiverer-RG*). While *Shiverer-Nscid* mice have a short life-span (~8-9 wks), *back crossing Shi mice into RG* resulted in a longer life span, up to ~14 weeks.

### Transplantation of HuCNS-SC

Neonatal mice (P1) were anesthetized using hypothermia and placed into a stereotaxic device (Cunningham mouse neonate stereotaxic adaptors, Harvard Apparatus) with a build in continuous cooling ice water circulator. With a light illumination, the sinus above lambda was identified as a reference point. To inject HuCNS-SC cells, burr holes were made in the skull cartilage by a 30 gauge needle and cell suspension was introduced by a Hamilton syringe with 33 gauge needle into the parenchyma. The following coordinates were used for neonatal transplant. Anteroposterior from midline (A), lateral from midline (L) and ventral from the surface of brain (V), respectively. The corpus callosum: (A, L, V): (2.0, 1.0, 1.0), with reference to Lambda. The fimbria of the fornix: (0.5, 1, 2.0) with reference to Lambda. The cerebellum: (-2.0, 0.8, -2.5), with reference to Lambda. HuCNS-SC cells were

transplanted bilaterally into the corpus callosum, fimbria of the fornix, and cerebellar white matter (100,000 cells per site), 600,000 cells per neonate. At each site, 100,000 HuCNS-SC cells in 1 microliter of cell suspension were introduced with a Hamilton syringe. After the procedure, animals were placed on a warming pad until revived, then returned to the mother until weaning.

Juvenile mice (21-27 days of age) were anesthetized with isoflurane and placed in the stereotaxic device. A small incision was made aseptically in the skin to expose the skull to visualize the cranial sutures. Cell suspensions (100,000 cells in 1  $\mu$ L at each site) were injected with a small gauge needle attached to a Hamilton syringe, bilaterally into the corpus callosum, the fimbria of the fornix, and cerebellar white matter. The following coordinates were used for juvenile transplant: the corpus callosum: (1.2, 1.2, -2.0) with reference to bregma. The Fimbria: (-1.0, 1.2 and -2.5) with reference to bregma. The cerebellum: (-2.0, 0.8 and -3.5) with reference to lambda. After the incision was closed, the mice were revived, monitored during recovery, and then returned to cages.

### **Immunohistochemical analysis of transplanted mouse brains**

Transplanted mice were anesthetized and perfused with PBS followed by 4% paraformaldehyde. Brains were serially sectioned (50  $\mu$ m) in the sagittal plane with a freezing microtome (Leica SM2400, Nussloch, Germany) and stained with various antibodies to reveal the distribution and morphology of transplanted cells (see Table S1, for list of antibodies). For immunoperoxidase staining with SC121 (STEM121, Stem Cell Sciences) and anti-MBP, brain sections were stained with primary antibodies, followed by biotinylated horse anti-mouse mAb (1:500, Vector Laboratory). Peroxidase

staining was visualized with an Elite ABC kit (Vector Laboratory) with NovaRed substrate (Vector Laboratory). Brain sections were mounted and counterstained with methyl green. Histological sections utilized in this study were imaged using an Olympus BX61 microscope.

### **Analysis of Node of Ranvier Formation**

Tissue sections were stained with antibodies to two proteins that flank the nodes of Ranvier: the paranodal contactin-associated protein (Caspr), a component of axo-glia junctions, and the potassium channel Kv1.2, situated in the juxtaparanodal region and which flanks the Caspr distribution. Tissue was pre-treated with antigen retrieval (100 mM Sodium Citrate pH 6.8; 80°C, 10 min) and blocked in PBS with 1.0% Triton X-100 and 5% NGS for 1 hour at room temperature (RT). Sections were incubated for 4 days at 4°C in PBS with 0.4% Triton X-100, 3% NGS, rabbit antiserum to Caspr (1:1000; a generous gift from Dr Elinor Peles, The Weizmann Institute of Science, Rehovot, Israel) and mouse anti-Kv1.2 monoclonal antibody (1:250; Clone K14/16; NeuroMab, Davis, CA). Secondary antibodies were incubated at RT for 2 hours: Alexa Fluor 568 goat anti-rabbit (1:500; A11036; Invitrogen), Alexa Fluor 488 goat anti-mouse (1:500; A11029; Invitrogen) and counterstained with Hoechst 33342 (1:3000, Invitrogen).

### **Electron Microscopy**

Following post-paraformaldehyde fixation in glutaraldehyde, brains were incubated in 0.1 M sodium cacodylate buffer overnight, fixed with osmic acid, washed in distilled water and dehydrated through a series of alcohols, immersed in propylene oxide, and embedded in Spurr resin. Semi-thin (1 µm) sections were stained with toluidine blue to aid in orientation of white matter tracts. Ultrathin sections (90 nm) were cut for regions

of interest, transferred to a 150 mesh copper grid, stained with uranyl acetate and lead citrate, and viewed on a Philips C10 transmission electron microscope.

### **Ex vivo high field strength magnetic resonance imaging**

Brains were collected from four neonatal animals that survived until 6 (n=2) or 7 weeks (n=2) and from four juvenile animals that survived until 5 (n=1), 6 (n=2) or 7 weeks (n=1). Brains were hemisected in the sagittal plane. Tissue was embedded alongside a corresponding control tissue block in 0.5% agarose and immersed in PBS within a 4 cm diameter plexiglass tube. A custom single-turn solenoidal coil (5 cm diameter, 5 cm length) was utilized for radiofrequency transmission and reception. Experiments were performed using an 11.7 T magnet interfaced with a 9 cm inner diameter magnetic field gradient coil (Bruker, Rheinstetten, Germany). Procedures generally followed the previously published strategy that used diffusion tensor imaging (DTI) to characterize postmortem tissue from other species. (46, 47).

A Stejskal-Tanner multi-slice spin-echo pulse sequence ( $\delta = 12$  ms,  $\Delta = 21$  ms, and  $G = 11.6$  G/cm; resulting in  $b = 2.5$   $\mu\text{s}/\text{mm}^2$ ) was used for DTI measurements. The  $b$ -value for this study was selected to provide an approximate match in diffusion sensitization to a typical *in vivo* measurement in which  $b = 1$   $\mu\text{s}/\text{mm}^2$  (the water apparent diffusion coefficient is  $\sim 2.5$ -fold smaller in post-mortem tissue than *in vivo*) (48). Diffusion anisotropy measurements were made using a 25-direction, icosahedral sampling scheme (49) in combination with two measurements in which  $b=0$ . Other pulse sequence settings were  $TR = 10$  s,  $TE = 42$  ms and NEX (the number of averaged transients) = 1. The image resolution was isotropic, with voxel dimensions of 0.2 mm and a 64 voxel (phase-encode) by 50 voxel (readout) by 384 voxel (slice-select) field of

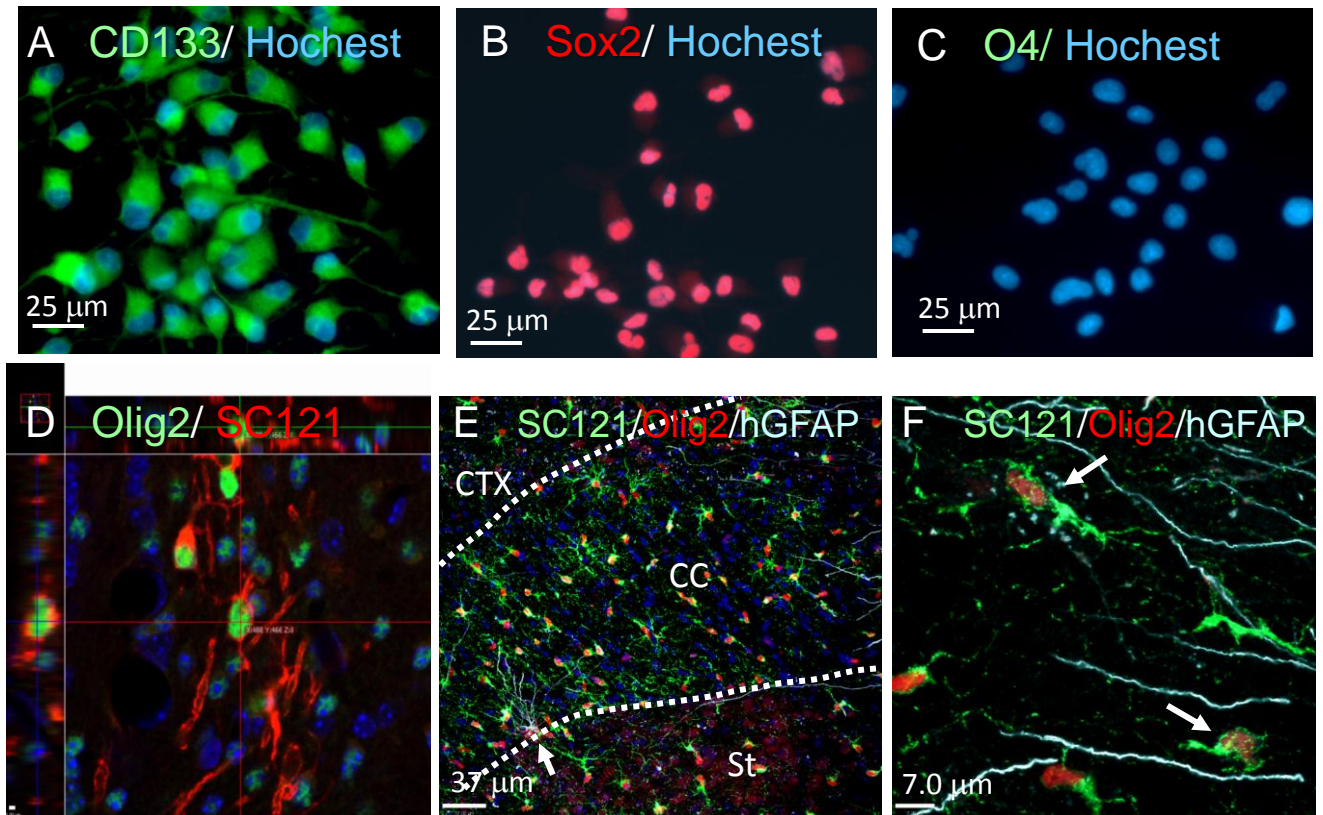
view. Standard procedures (49) were followed to determine eigenvalues ( $\lambda_1$ ,  $\lambda_2$ , and  $\lambda_3$ , listed from smallest to largest) and the signal amplitude in the absence of diffusion weighting (the “b=0” image) for each voxel from the set of 27 3D images. Fractional anisotropy (FA, defined in (50)) was calculated from the eigenvalues for each voxel.

The b=0 images from the DTI data provided sufficient T<sub>2</sub>-based image contrast to define cerebellar white matter regions of interest (ROIs) (Fig. 8 and Supplemental Fig. 7). These T<sub>2</sub>-weighted images were bias corrected using 3D Slicer and Matlab (The Mathworks, Natick, MA, USA). Each scan was first bias corrected using 3D slicer's MRI bias field correction (N3 algorithm, Shrink Factor = 3, Max Iterations = 30, Fit levels = 3, Weiner Filter = 0.1, Full Width = 0.7, Conv. Threshold = 0.001) (51-53) Note that the bias field correction was only applied to images used to delineate ROI boundaries and was not applied to images in subsequent analyses. The resulting images were then normalized to one another in Matlab using agar as a consistent point of reference. Each brain was rotated to the histological x/y axis using functionalities in Matlab and the FMRIB Analysis Group software (FSL)

**Table S1**  
**Antibodies used for histological and immunohistochemical studies**

Antibody	Host	Dilution	Source	Specificity
Caspr	Rabbit	1:1000	Dr. Elior Peles	Caspr
CC-1/APC	Mouse	1:100	Calbiochem	Mature Oligodendrocytes
Kv1.2	Mouse	1:250	NeuroMab	Clone k14/16
Ki67	Rabbit	1:500	Epitomics	Proliferating cells
hNCAM	Mouse	1:100	Caltag	Human neurons
hNestin	Mouse	1:4000	R&D Systems	Human neural progenitors
MBP	Mouse	1:5000	Covance	Myelinating Oligodendrocytes
NeuN	Mouse	1:500	Millipore	Mature Neuronal cells
Olig2	Rabbit	1:20,000	Dr. John Alberta	Pan-Oligodendrocyte marker
Olig2	Goat	1:1000	R&D Systems	Pan-Oligodendrocyte marker
S100b	Rabbit	1:10,000	Swant	Astrocytes
SC101 (STEM101™)	Mouse	1:200	Stem Cell Science	Human Nucleus
SC121 (STEM121™)	Mouse	1:1000	Stem Cell Science	Human Cytoplasm
SC123 (STEM123™)	Mouse	1:3000	Stem Cell Science	Human GFAP

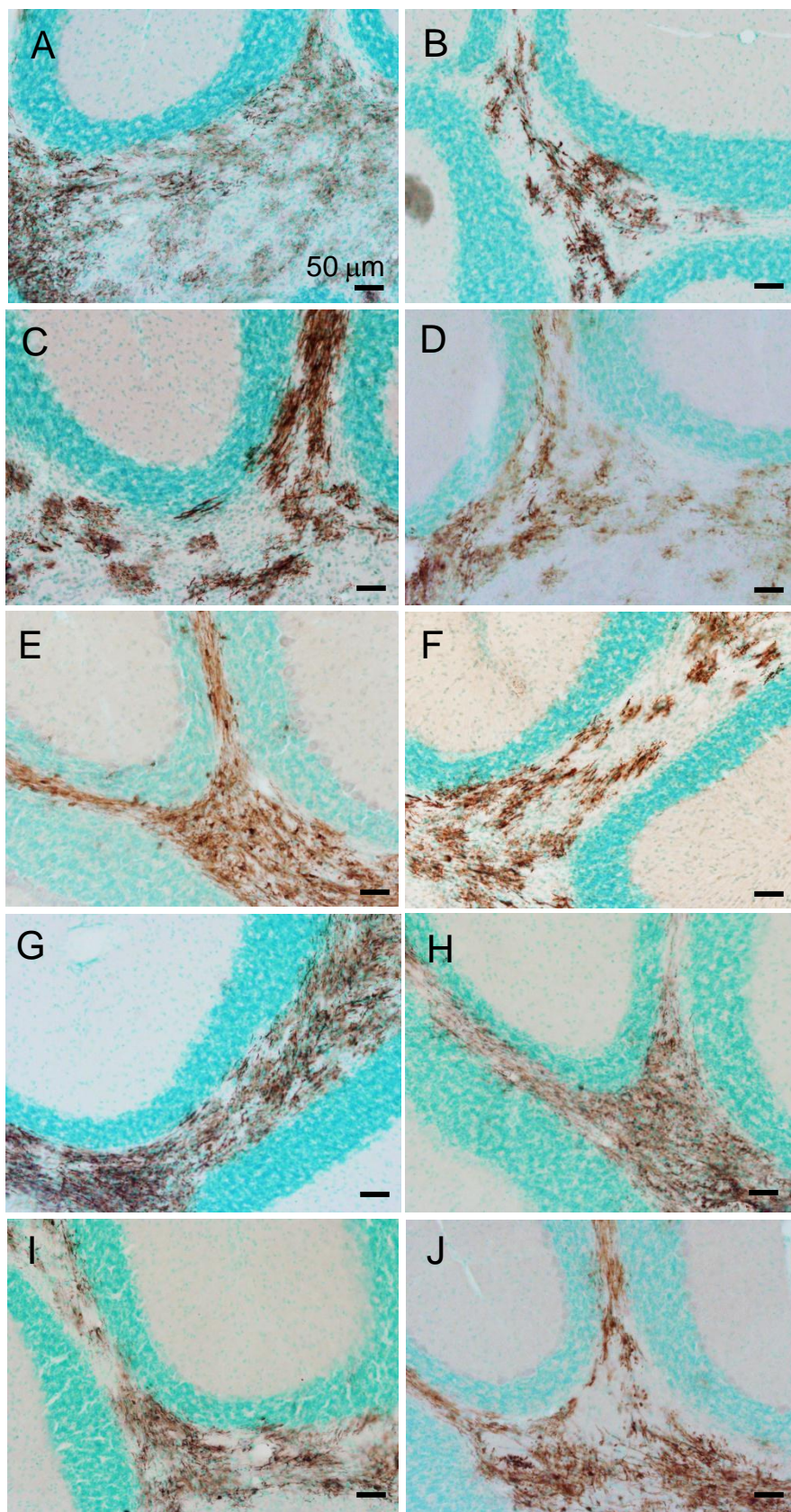
Fig. S1



**Supplemental Figure 1**

HuCNS-SC characteristics before and after transplantation. HuCNS-SC express (A) CD133 (green) . (B) Sox2 (red), but not (C) O4 (green). Nuclear counterstain with Hoechst 33324 (blue). (D) Confocal Z-stack analysis of cells stained for Olig2 (green) and SC121 (red), as shown in Figure 2A, confirmed the commitment of the SC121+ cells to the oligodendrocyte lineage. (E,F) Confocal analysis in the corpus callosum of cell fate commitment of HuCNS-SC transplantation into a heterozygote *Shi-id* mouse at 25 weeks post transplant. Sections were triple stained with antibodies against SC121 (green), Olig2 (red) and hGFAP (SC123, light blue); Hoechst 33324 nuclear counterstain (dark blue). The boundary between the corpus callosum (CC) and cortex (CTX) or Striatum (St) is delineated with the white dotted lines. A rarely visualized human astrocyte defined by hGFAP is indicated (arrow). (F) a higher magnification image of the corpus callosum. Adjacent to this the astrocyte processes (light blue) several human Olig2+SC121+ cells committed to the oligodendrocyte lineage (arrows).

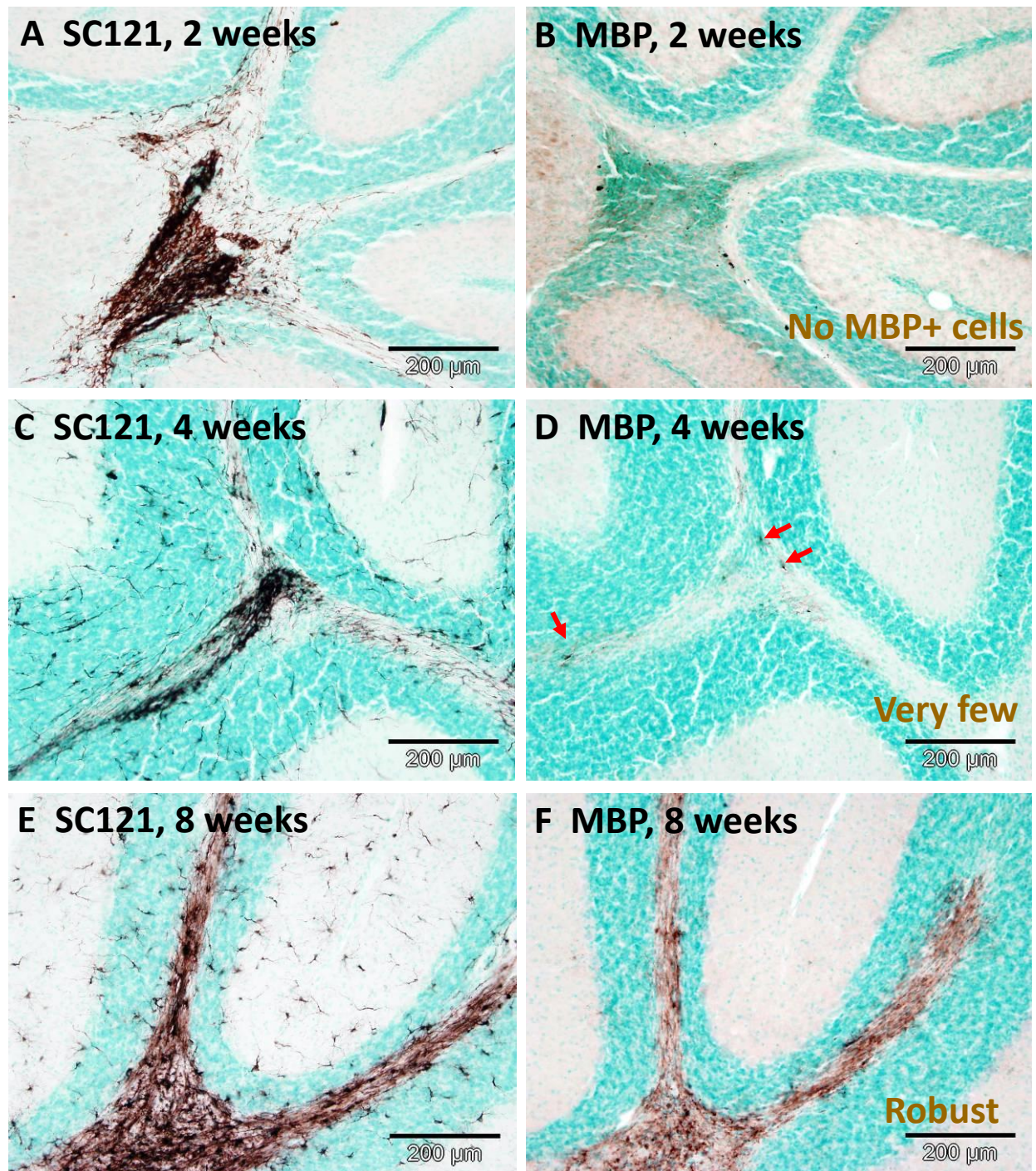
Fig. S2



**Supplemental Figure 2**

Production of myelin from 10 different HuCNS-SC lots. MBP staining in the cerebellum of transplanted *Shi-id* mouse brains from 10 different HuCNS-SC lots studied at the indicated times after transplantation into neonates (A, D-J) and juveniles (B,C): (A) 42, (B) 42,(C) 43, (D) 44, (E) 47, (F) 49, (G) 56, (H) 57, (I)58, and (J) 60 days.

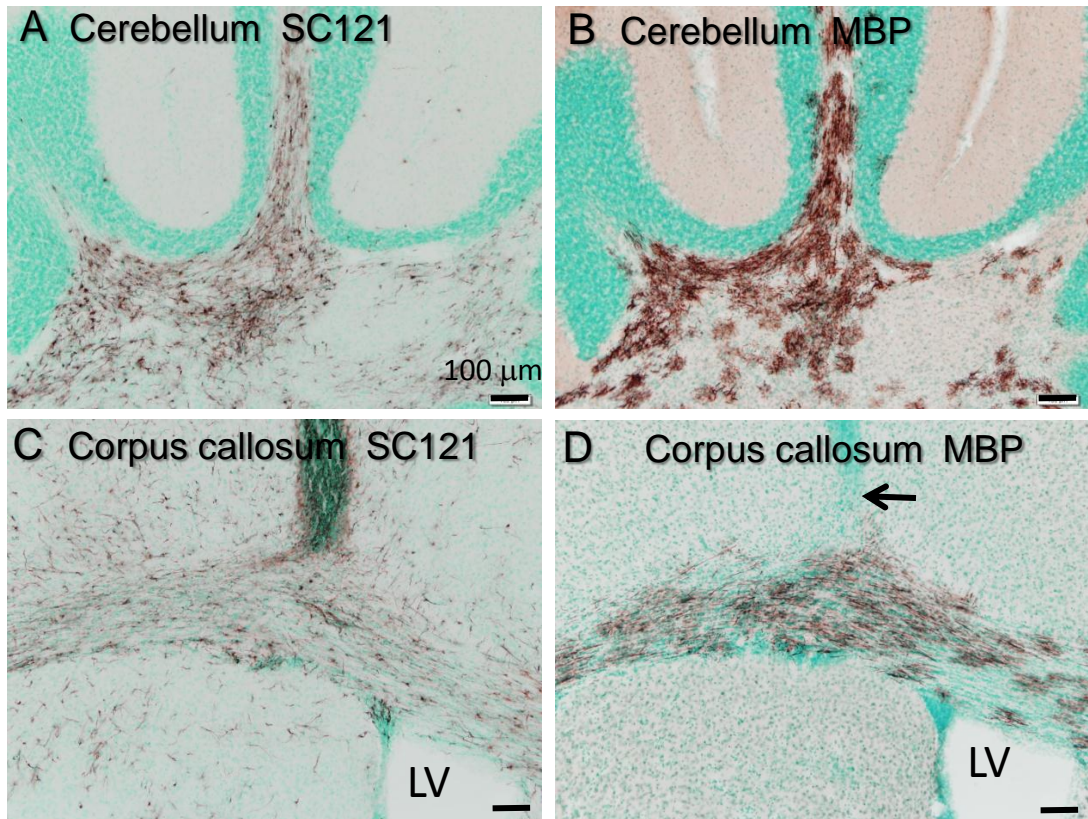
Fig. S3



### Supplemental Figure 3

Time course of HuCNS-SC engraftment and oligodendrocyte differentiation in vivo. Transplanted cells migrated from the implantation site as early as 2 weeks post-transplantation (A), but did not stain with anti-MBP antibody (B). The human cells migrated more extensively 4 weeks post-transplantation (C) and low numbers of human MBP<sup>+</sup> cells were visualized (D, arrows). By 8 weeks after transplantation, the human cells migrated throughout the white matter tracts and into other cell layers of the cerebellum (E). Dense production of myelin produced by human oligodendrocytes is indicated by staining for MBP (F).

Fig. S4



**Supplemental Figure 4**

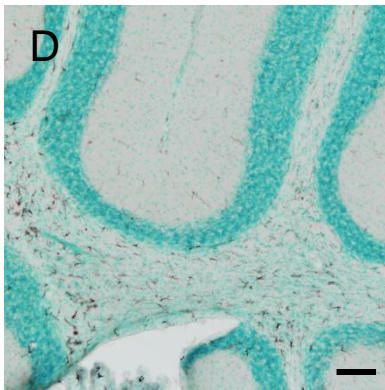
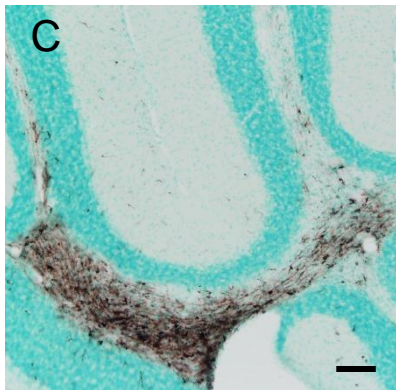
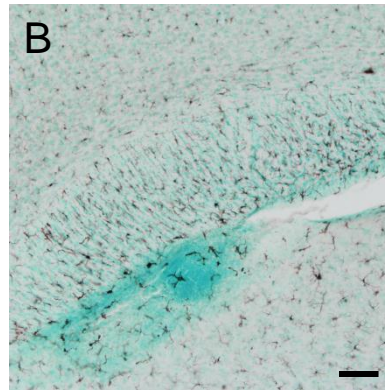
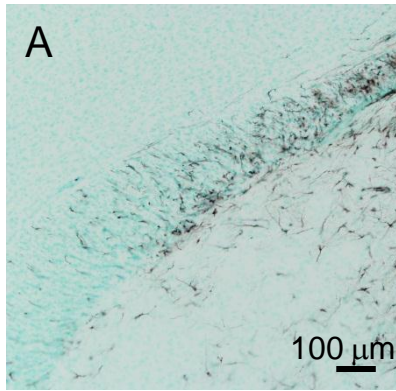
Juvenile transplantation of HuCNS-SCs: engraftment and migration of HuCNS-SC into white matter tracts with site specific oligodendrocyte differentiation. (A) SC121 staining visualized diffuse engraftment of human cells throughout the cerebellar white matter tracts at 6 weeks post transplant. (B) In an adjacent section to that shown in A, robust MBP staining was observed exclusively in the cerebellar white matter. (C) Similar to the cerebellar transplants, diffuse engraftment of human cells was detected by SC121 in the corpus callosum at 10 weeks after transplantation. (D) Diffuse MBP staining was visualized in a section adjacent to that shown in C. No MBP staining in the bolus (arrow)

Fig. S5

Neonatal transplantation

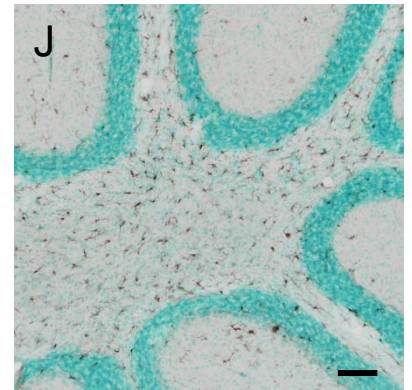
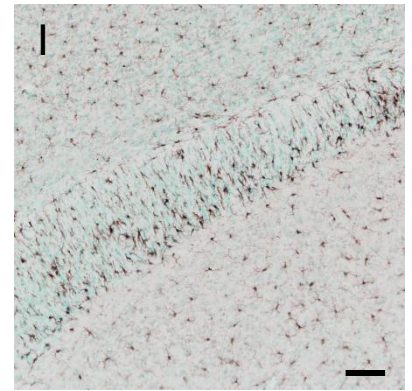
SC121

Iba1



NT *Shi-id*

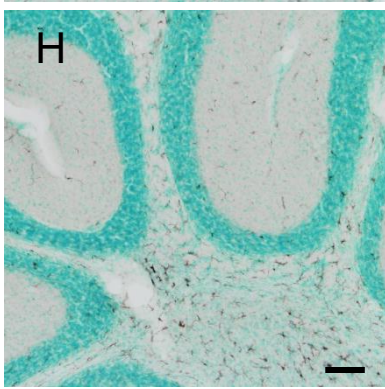
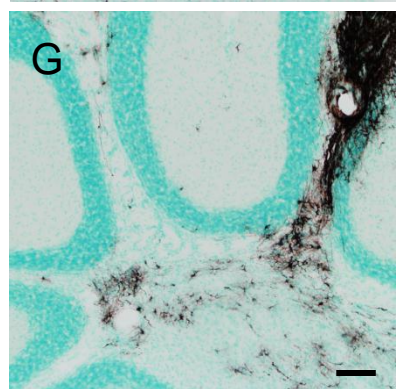
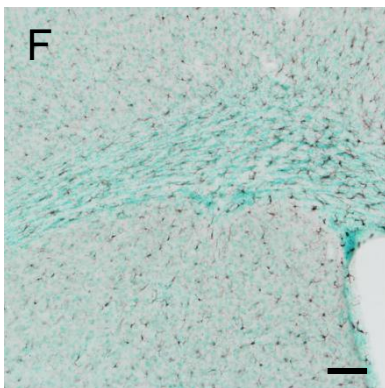
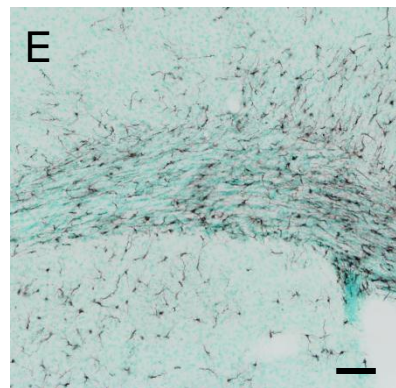
Iba1



Juvenile transplantation

SC121

Iba1



NT *id*

Iba1

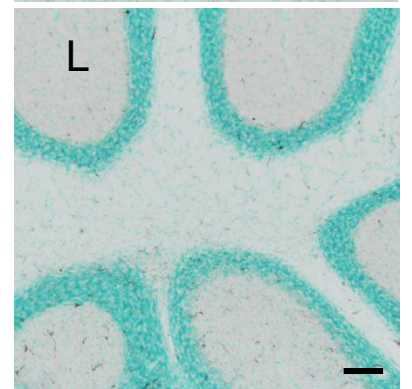
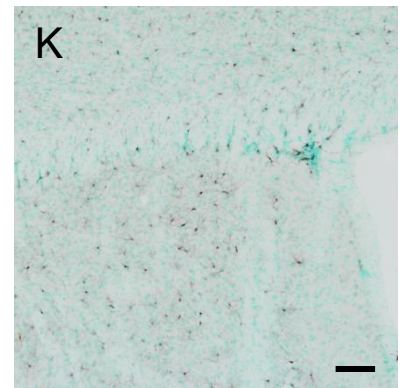
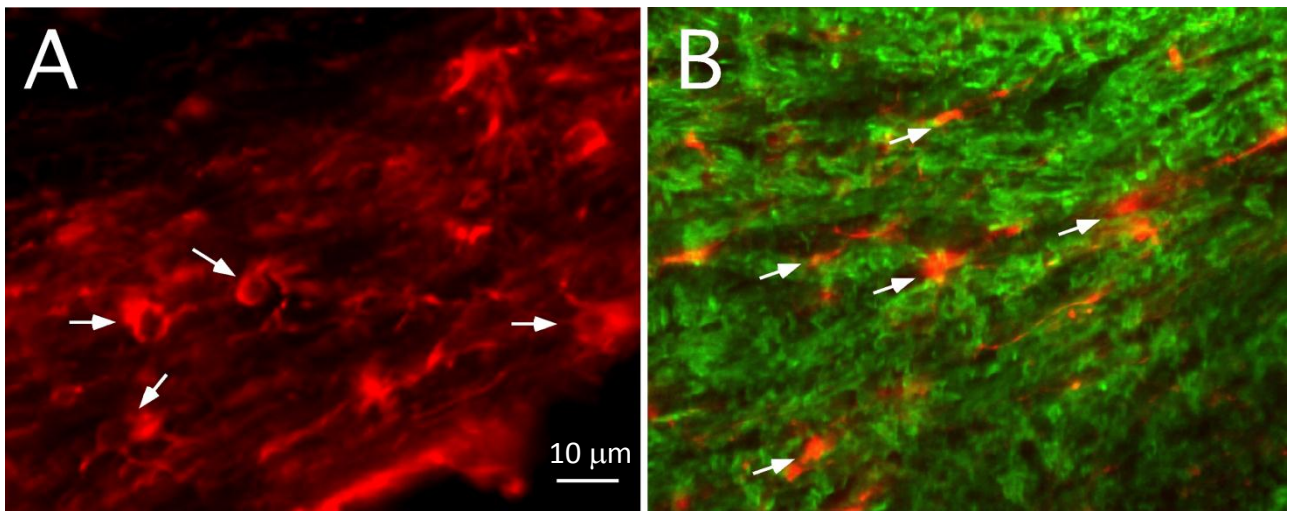


## Fig. S5 (cont.)

### **Supplemental Figure 5**

Microglia activation status of chronic transplants in *Shi-id* mouse brains. Immunoperoxidase staining with SC121 (A, C, E, G), and Iba1 (B, D, F, H) detected human engraftment and microglia, respectively, as visualized in sibling brain sections from neonatal (10 weeks post-transplant) (A-D) and juvenile (11 weeks post-transplant) (E-H) *Shi-id* mice. Iba-1 staining of age-matched (10 weeks of age) non-transplanted (NT) *Shi-id* mice (I, J) revealed no apparent difference in the distribution or morphology of the microglia compared to transplanted animals (B, D, F, H). Non-transplanted (NT) *id* mouse controls (K, L), i.e., wild type for shiverer mutation, displayed markedly less Iba-1 immunoreactivity, which supports that the more pronounced microglial staining is related to the Shiverer phenotype rather than the chronic transplants.

Fig. S6

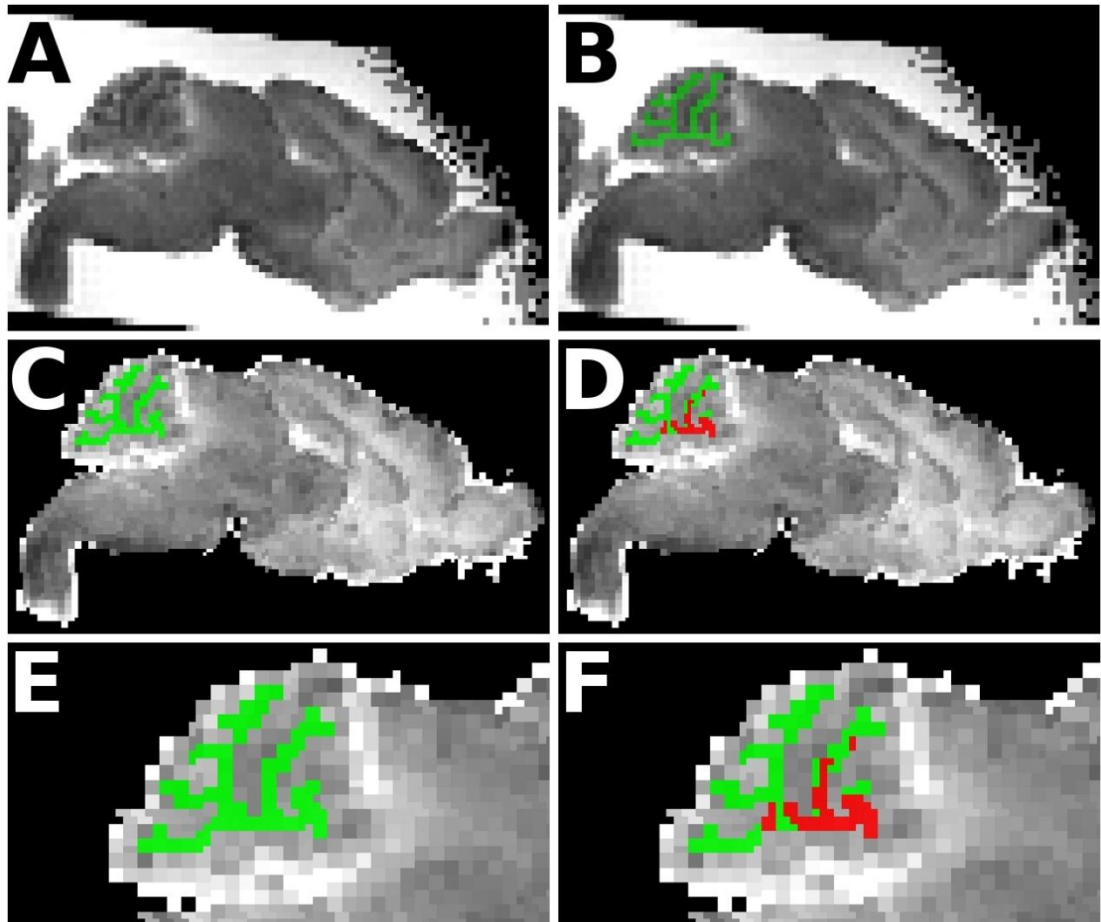


**Supplemental Figure 6**

Compound action potential (CAP) recordings were done in regions of humanized myelination of the corpus callosum (CC) of *Shi-id* mice injected with HuCNS-SC.

(A, B) Immunohistochemistry of a CC slice after CAP recording demonstrates the presence of MBP-immunoreactive human stem cells (red, A, B) that were closely associated with neurofilament-immunoreactive axons (green, B).

Fig. S7



**Supplemental Figure 7.**

Representative MRI study showing the approach used to define cerebellar white matter tracts and regions of human myelination in the Shi-id mouse transplanted with HuCNS-SC. (A) Low power parasagittal T<sub>2</sub> map at one level of the entire brain from a neonatal animal at 6 weeks after transplantation. (B) A white matter segmentation (green) was generated based upon the T<sub>2</sub> map in A. (C) View of the image in B after it has been rotated in the sagittal plane to be co-planar with the histological plane of section. (D) Superimposed on the white matter ROI in C are the regions corresponding to an absence of myelination (green) or to human myelination (red) as defined by the montages of MBP staining (e.g., see Fig. 7C). (E) Detailed view of panel C. (F) Detailed view of panel D.